Article

Optimal Adaptive Gain LQR-based Energy Management Strategy for Battery-Supercapacitor Hybrid Power System

Seydali Ferahtia [1,*], Ali Djeroui [2], Tedjani Mesbahi[3], Azeddine Houari[4], Samir Zeghlache[1], Hegazy Rezk[5] and Théophile Paul[3]

[1] Laboratoire d'Analyse des Signaux et Systémes dept of electrical engineering. University of M'sila. Algeria ; sidali.ferahtia@univ-msila.dz
[2] Electrical Engineering Laboratory dept. of electrical engineering. University of M'sila. Algeria ; ali.djeroui@univ-msila.dz
[3] ICube CNRS (UMR 7357) INSA Strasbourg, University of Strasbourg, F-67000 Strasbourg, France
[4] IREENA Laboratory, University of Nantes, Saint-Nazaire, France
[5] College of Engineering at Wadi Addawaser, Prince Sattam BinAbdulaziz University, Al-Kharj, Kingdom of Saudi Arabia and Electrical Engineering, Minia University, Egypt.
* Correspondence: e-mail@e-mail.com; Tel.: (optional; include country code; if there are multiple corresponding authors, add author initials)

Abstract: This paper aims at presenting an energy management strategy (EMS) based upon optimal control theory for a battery-supercapacitor hybrid power system. The hybrid power system consists of a Lithium-ion battery and a supercapacitor with associated bidirectional DC/DC converters. The proposed EMS aims at computing adaptive gains using salp swarm algorithm and load following control technique to assign the power reference for both the supercapacitor and the battery while achieving optimal performance and stable voltage. The DC-DC converter model is derived utilizing the first-principles method and compute the required gains to achieve the desired power. The fact that the developed algorithm takes disturbances into account increases the power elements' life expectancies and supplies the power system with the required power

Keywords: Battery; Supercapacitor; Hybrid power system; Optimal control; DC/DC converter; Energy management strategy

1. Introduction

Nowadays, with the expansion of the energy crisis and ecological pollution, hybrid power systems (HPSs) are becoming a strategic solution. Hybrid power systems (HPSs) are a set of co-operating power sources, the coordination of their operation is realized by means of advanced power electronics systems [1]. Due to its advantages, the HPS can be employed for the EVs applications [2–4] or for the stationary applications [5–7]. This resulted in a spark of interest in the research field, with different hybridizations and energy management strategies having been developed to further reduce emissions and improve fuel economy [8].

Battery - supercapacitor HPS is getting more attention due to its superior performance and simplicity of control. The Lithium battery, despite having a high-energetic density, doesn't yield a high enough power density while the opposite can be said about the supercapacitor. A hybridization thus proves suitable to increase both components lifetime and improve the overall performance, especially considering storage elements' states of charge and temperatures. Using of the supercapacitor in the case of sudden load variations is an example. In addition to that, high-frequency disturbances negatively impact the battery's life expectancy, which can be alleviated by the supercapacitor due to its characteristics. The main challenge is to provide a suitable energy management strategy (EMS) which takes all of these factors into account to provide optimal performance while considering different constraints.

Preprints (www.preprints.org) | NOT PEER-REVIEWED | Posted: 19 January 2021 doi:10.20944/preprints202101.0371.v1

Various methods concerning the energy management of a hybrid power system have been reported in the literature [9–11]. They are generally divided into a group of three main methods: optimization-based methods, rule-based methods or more recently learning-based methods. Figure 1 showcases the three main categories of energy management strategies and some of the methods involved.

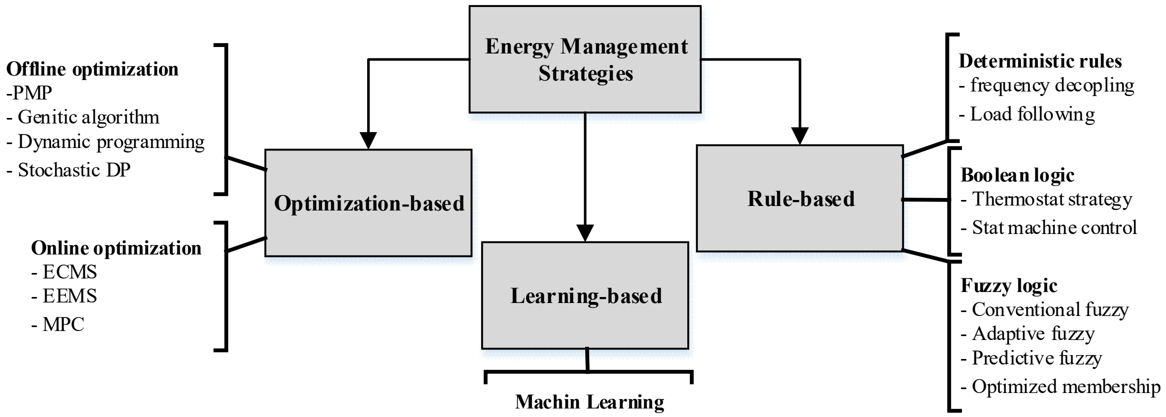

Figure 1. The most common EMSs.

Optimization-based methods make use of the tools provided by optimization theory to solve the problem at hand, the latter being an optimal distribution of the load power amongst the battery/supercapacitor hybrid system such that it improves upon their life expectancies given their respective constraints (state of charge, supercapacitor voltage for instance.)

A subsidiary of optimization-based methods is online optimization: it is applicable in a real-time scenario, such as computing the optimal distribution of energy amongst a hybrid system given the power load. Methods such as Model Predictive Control (MPC), Equivalent Consumption Minimization Strategy (ECMS) can be qualified as online optimization methods.

Rule-based methods, on the other hand, can be summed into a series of IF-THEN scenarios. State machine and thermostat control can both be achieved easily and implemented in the real-time scenario. Another method is to use a fuzzy logic controller, which proves quite robust and makes its decision regarding the power distribution dependent of the output of its membership functions and can be easily tuned to achieve optimal operation. The main drawback of these methods is that the elaboration of said rules requires knowledge and past experience of an expert, which is not always available.

Learning-based methods make use of the recent advancements regarding Machine Learning (ML), a sub-field of Artificial Intelligence (AI), which has seen a surge in its use over the last decade. It has proven to yield excellent results in some fields, especially in image classification, hence its extensive use in some other fields, including energy management. A model has to be trained using a database, which is not always available. This can prove quite difficult, notably because not enough research has been done in this relatively recent field. Another drawback is the fact that it has no guarantee to work for data outside the one used for training.

Despite their use in some cases [12,13], none of these strategies combined the advantages procured by the frequency decoupling approach and optimization-based strategies. The proposed method overcomes some of the drawbacks of the frequency decoupling technique while providing the benefits of optimization-based methods, thus improving the overall HPS performance.

The proposed method consists of combining the frequency decoupling (FD) approach with an optimal control by using a Linear Quadratic Regulator (LQR) in order to

 doi:10.20944/preprints202101.0371.v1

compute the control gains which will be updated by means of salp swarm algorithm. The models used in simulations have been achieved through a literature review [14,15].

In order to distribute the required power between the two energy sources, a load following strategy (LFS) is adopted. The bus voltage will be stabilized by the supercapacitor due to its fast dynamics while the battery will handle the load power and the supercapacitor required power. The main contribution comes from the usage of both a lower-level control architecture as well as a higher-level one, which allows improving energy quality while diminishing the strains on the power sources, thus achieving a higher life cycle.

The main contributions of the paper are summarized below:

- Robust control ensures good energy quality provided to the load side and an extended HESS components lifetime.
- Validations done through simulation and experimentation
- Combination of different methods to achieve an optimal performance

2. HPS Topology Structure and Modeling

Batteries have the characteristics of high-energy density and relatively low power density. Moreover, the internal resistance could increase when the battery operates with high-frequency loads, which lead to its degradation. The supercapacitor is a high power density with a high number of charging/discharging cycles. Thus, the combination of battery and supercapacitor can provide a complementary advantage to meet the load demand [16].

In the literature, passive, semi-active and active topologies have been reported. Each one has its characteristics. Figure 2 illustrates these topologies.

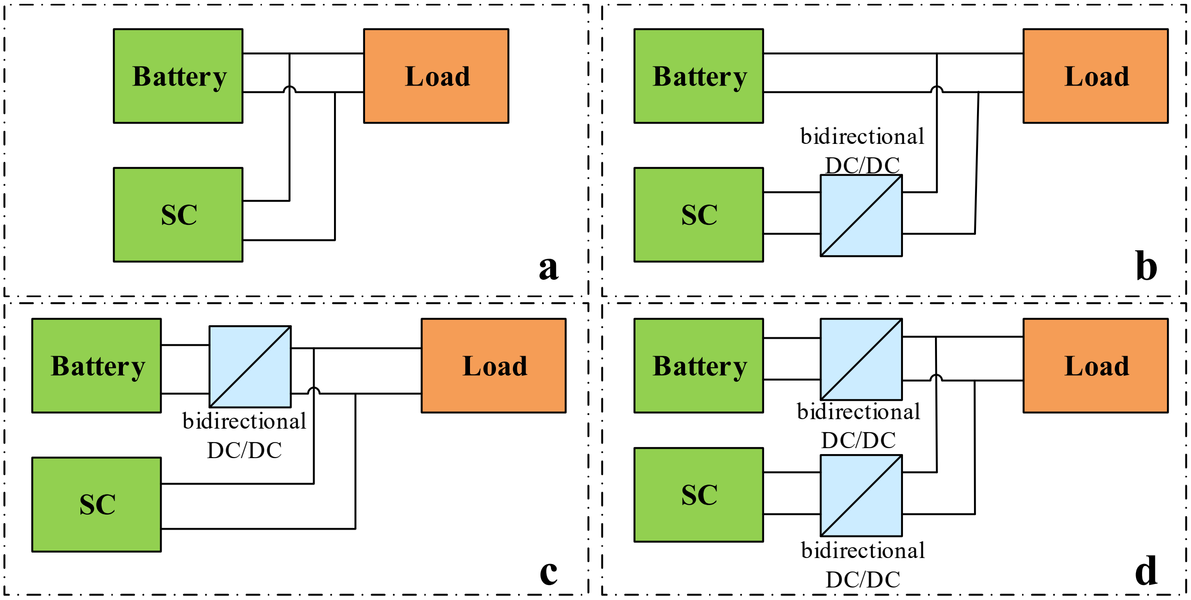

Figure 2. HPS topologies: (**a**) passive topological structure; (**b**) semi-active topology; (**c**) Another type of semi-active topology; (**d**) fully active topology.

As displayed in Figure 3(a), the configuration of the studied HPS is based on fully active topology. The electrical power system is comprised of a supercapacitor and a Lithium battery, each one of them connects the DC bus through bidirectional DC/DC converters to power the load as detailed in Figure 3(b). In this system, the proposed EMS is based on optimal power-sharing method (LQR) that calculates the references to the low-level controllers in order to satisfy the load demand while a high-level control minimizes the DC bus overshoots under step loads.

Preprints (www.preprints.org) | NOT PEER-REVIEWED | Posted: 19 January 2021 doi:10.20944/preprints202101.0371.v1

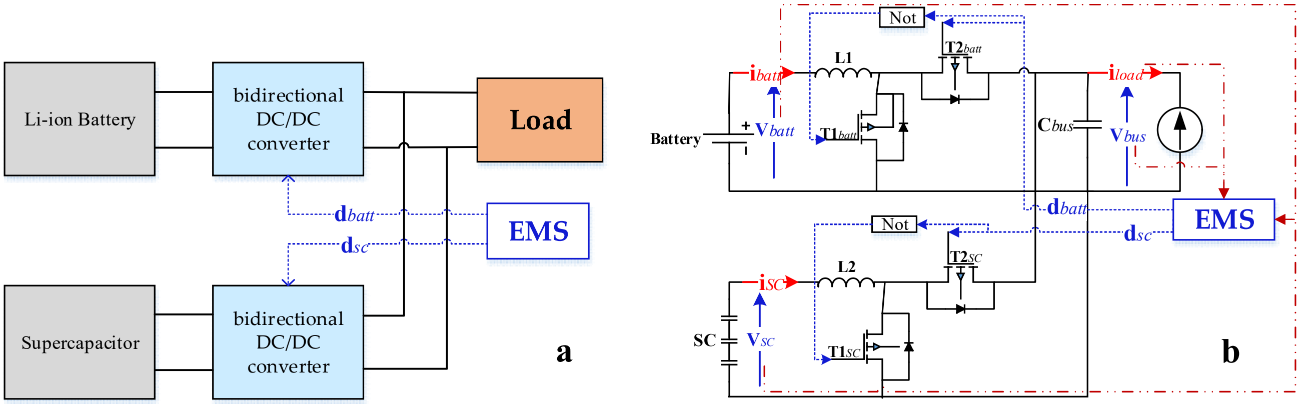

Figure 3. Studied system: **(a)** overview of the system; **(b)** Electrical circuit of the considered system.

In this paper, a Li-ion battery is selected as a principal source due to their proven efficiency and high energy density as opposed to other battery technologies. A model available in MATLAB's SPS (SimPowerSystems) Toolbox is considered in order to validate by simulation the proposed EMS. The battery model depicted in Figure 2 is based on the Thévenin circuit. This battery model is detailed in [17]. The battery voltage is expressed as follows:

$$V_{batt} = E_0 - K\frac{Q}{Q-i_t} - R_b i + A_b e^{(-Bi_t)} - K\frac{Q}{Q-i_t} i^* \tag{1}$$

Where Vbatt is the battery voltage. E0 is the battery constant voltage (V). K is the polarization constant (V/Ah). Q is the battery capacity (Ah). i* is the filtered battery current (A). it is the actual battery charge (Ah). Ab is the exponential zone amplitude (V). B is the exponential zone time constant inverse (Ah^(-1)) and Rb is the battery internal resistance (Ω). As for the polarization resistance Polres, which is only present when charging the battery, it is expressed as follows:

$$Pol_{res} = K\frac{Q}{i_t - 0.1Q} \tag{2}$$

The detailed battery scheme is given in figure 4.

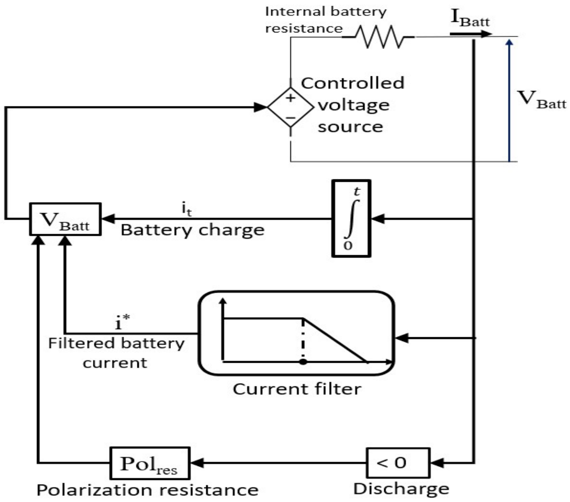

Figure 4. Li-ion battery model.

Preprints (www.preprints.org) | NOT PEER-REVIEWED | Posted: 19 January 2021 doi:10.20944/preprints202101.0371.v1

Supercapacitors, despite not being to withhold as much energy as Li-ion batteries, are able to release energy at a faster rate due to their high dynamics. The considered model also comes from MATLAB's SPS Toolbox, where more details can be found in [4]. The supercapacitor output voltage V_SC expression is given as follows:

$$V_{SC} = \frac{Q_T}{C_T} - R_{SC} i_{SC} \tag{3}$$

Where Q_T is the total electric charge (Coulombs), C_T is the supercapacitor module capacitance, R_{SC} is the supercapacitor module resistance (Ω) and i_{SC} is the supercapacitor module current (A). It is dependent of the supercapacitor's state of charge. The supercapacitor block is given in Figure 5.

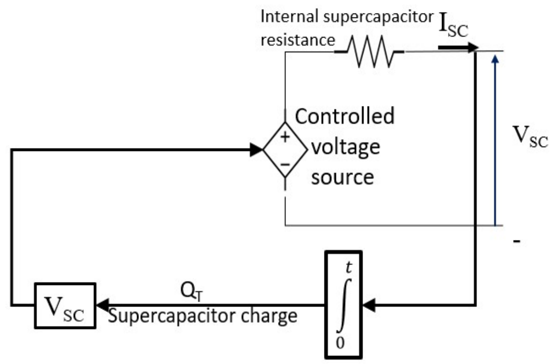

Figure 5. Supercapacitor model.

Two main models are used throughout the literature: the switching model and the average one. The average model proves sufficient for this case. The switching models are mainly used for design purposes and to investigate types of pulse-width-modulated schemes with regard to switching harmonics and losses. These models require low sampling time to observe all the switching actions, which makes the simulation very time consuming, hence the choice of an average model for this paper.

$$\begin{cases} L_1 \dfrac{di_{batt}}{dt} = V_{batt} - V_{bus} d_{batt} - R_{batt} i_{batt} \\ L_2 \dfrac{di_{SC}}{dt} = V_{SC} - V_{bus} d_{SC} - R_{SC} i_{SC} \\ C_{bus} \dfrac{dV_{bus}}{dt} = d_{batt} i_{batt} + d_{SC} i_{SC} - i_{bus} \end{cases} \tag{4}$$

3. The Proposed EMS

The proposed EMS is based load following strategy (LFS). It possesses two main components: a lower-level controller and a higher-level one. The power reference for each source is generated higher-level, while the lower-level one compensates for the DC bus current fluctuations, ensuring an optimal performance paired with an overall better energy quality. The operating control scheme is illustrated in Figure 6.

At the higher-level EMS. The supercapacitor power regulates the DC bus voltage and handles the high-frequency power. The DC power reference is generated based on the DC bus voltage, where an LQR is used to stabilize it. The available bus energy can be expressed as

Preprints (www.preprints.org) | NOT PEER-REVIEWED | Posted: 19 January 2021 doi:10.20944/preprints202101.0371.v1

$$\frac{dE_{bus}}{dt} = P_{SC} + P_{batt} - P_{load} \tag{5}$$

Where E_{bus} is the bus energy, P_{load}, P_{SC}, P_{batt} is the load, supercapacitor and battery power respectively. The supercapacitor power reference can be obtained as

$$P_{SC}^{ref} = \frac{dE_{bus}}{dt} + P_{load} - P_{batt} \tag{6}$$

Where required power by the bus can be obtained using LQR controller.

The battery mainly feeds the load and maintains the DC voltage at the reference value. LQR controller is used for generating the SC required power. The control law can be written as

$$P_{batt}^{ref} = P_{SC}^{req} + P_{load} \tag{7}$$

Where the supercapacitor required is generated by an LQR controller.

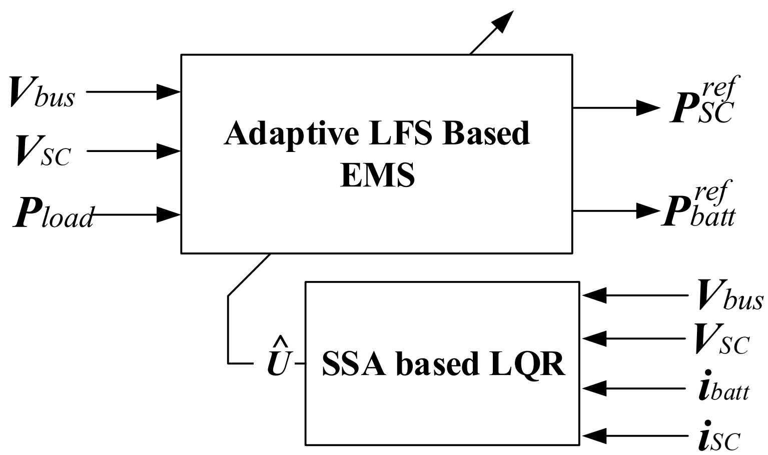

Figure 6. Adaptive LFC based EMS.

The lower level generates the duty cycle for each converter, based on the generated power references. The current references will be generated and compared with the measured ones. The regulation process will be achieved using current LQR. The adaptation of the controller parameters will be realized by means the SSA real-time optimizer. The detailed control scheme is described in Figure 7.

The LQR (Linear Quadratic Regulator) is an optimal controller that is used extensively due to its solid performances. It relies upon the minimization of the cost function

$$J = \int_0^\infty (\mathrm{x}^T \mathrm{Q} \mathrm{x} + u^T \mathrm{R} \mathrm{u})\, \mathrm{dt} \tag{8}$$

A state feedback control U= -Kx(t), U being the control input, x(t) the state vector and K=R^(-1) B^T S is the gain matrix defined as

$$K = R^{-1} B^T S \tag{8}$$

While S is the symmetric positive definite solution to the algebraic Riccati equation:

$$Q + A^T S + SA - SB(\mathrm{R}^{1-})\,\mathrm{B}^T\, S = 0 \tag{9}$$

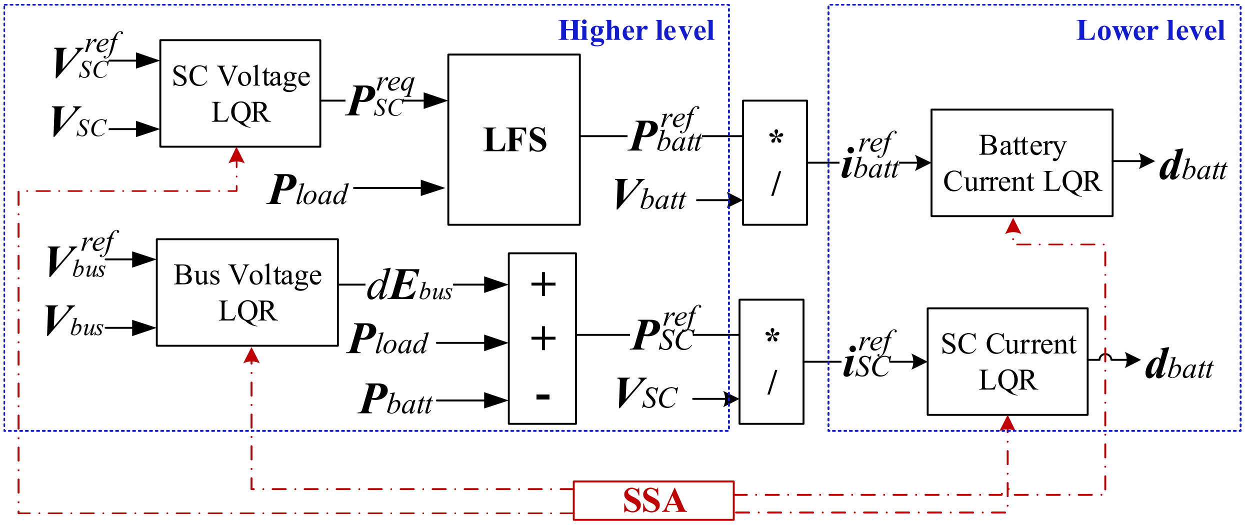

Figure 7. The Detailed EMS Scheme.

3.1. LQR Controller

Q and R are symmetric positive definite weighing matrices. They are chosen depending on the desired closed loop performance, the Q matrix penalizing the states while the R matrix penalizes the actuators. An augmented system regrouping the battery and supercapacitor's voltage and currents is given:

$$\begin{bmatrix} \dot{x}_1 \\ \dot{x}_2 \\ \dot{x}_3 \\ \dot{x}_4 \\ \dot{x}_5 \\ \dot{x}_6 \\ \dot{x}_7 \\ \dot{x}_8 \end{bmatrix} = \begin{bmatrix} 0 & 1 & 0 & 0 & 0 & 0 & 0 & 0 \\ 0 & \frac{-1}{\tau_1} & 0 & 0 & 0 & 0 & 0 & 0 \\ 0 & 0 & 0 & 1 & 0 & 0 & 0 & 0 \\ 0 & 0 & 0 & \frac{-1}{\tau_2} & 0 & 0 & 0 & 0 \\ 0 & 0 & 0 & 0 & 0 & 1 & 0 & 0 \\ 0 & 0 & 0 & 0 & 0 & \frac{-1}{\tau_3} & 0 & 0 \\ 0 & 0 & 0 & 0 & 0 & 0 & 0 & 1 \\ 0 & 0 & 0 & 0 & 0 & 0 & 0 & \frac{-1}{\tau_4} \end{bmatrix} \begin{bmatrix} x_1 \\ x_2 \\ x_3 \\ x_4 \\ x_5 \\ x_6 \\ x_7 \\ x_8 \end{bmatrix} + \begin{bmatrix} 0 & 0 & 0 & \\ \frac{-k_1}{\tau_1} & 0 & 0 & 0 \\ 0 & 0 & 0 & 0 \\ 0 & \frac{-k_2}{\tau_2} & 0 & 0 \\ 0 & 0 & 0 & 0 \\ 0 & 0 & \frac{-k_3}{\tau_3} & 0 \\ 0 & 0 & 0 & 0 \\ 0 & 0 & 0 & \frac{-k_4}{\tau_4} \end{bmatrix} \begin{bmatrix} U_1 \\ U_2 \\ U_3 \\ U_4 \end{bmatrix} \tag{10}$$

Preprints (www.preprints.org) | NOT PEER-REVIEWED | Posted: 19 January 2021 doi:10.20944/preprints202101.0371.v1

$$Q=\begin{bmatrix} q_{11} & 0 & 0 & 0 & 0 & 0 & 0 & 0 \\ 0 & q_{22} & 0 & 0 & 0 & 0 & 0 & 0 \\ 0 & 0 & q_{33} & 0 & 0 & 0 & 0 & 0 \\ 0 & 0 & 0 & q_{44} & 0 & 0 & 0 & 0 \\ 0 & 0 & 0 & 0 & q_{55} & 0 & 0 & 0 \\ 0 & 0 & 0 & 0 & 0 & q_{66} & 0 & 0 \\ 0 & 0 & 0 & 0 & 0 & 0 & q_{77} & 0 \\ 0 & 0 & 0 & 0 & 0 & 0 & 0 & q_{88} \end{bmatrix}, \mathrm{R}=\begin{bmatrix} r_{11} & 0 & 0 & 0 \\ 0 & r_{22} & 0 & 0 \\ 0 & 0 & r_{33} & 0 \\ 0 & 0 & 0 & r_{44} \end{bmatrix} \tag{11}$$

$$S=\begin{bmatrix} S_{11} & S_{12} & S_{13} & S_{14} & S_{15} & S_{16} & S_{17} & S_{18} \\ S_{21} & S_{22} & S_{23} & S_{24} & S_{25} & S_{26} & S_{27} & S_{28} \\ S_{31} & S_{32} & S_{33} & S_{34} & S_{35} & S_{36} & S_{37} & S_{38} \\ S_{41} & S_{42} & S_{43} & S_{44} & S_{45} & S_{46} & S_{47} & S_{48} \\ S_{51} & S_{52} & S_{53} & S_{54} & S_{55} & S_{56} & S_{57} & S_{58} \\ S_{61} & S_{62} & S_{63} & S_{64} & S_{65} & S_{66} & S_{67} & S_{68} \\ S_{71} & S_{72} & S_{73} & S_{74} & S_{75} & S_{76} & S_{77} & S_{78} \\ S_{81} & S_{82} & S_{83} & S_{84} & S_{85} & S_{86} & S_{87} & S_{88} \end{bmatrix} \tag{12}$$

The control law U becomes:

$$U = R^{-1}B^{T}Sx = -Kx \tag{13}$$

With

$$\begin{cases} U_1 = k_I^{i_{SC}} \int (\mathrm{i}_{SC}^{ref} - \mathrm{i}_{SC})\,\mathrm{dt} + k_P^{i_{SC}} (\mathrm{i}_{SC}^{ref} - \mathrm{i}_{SC}) \\ U_2 = k_I^{i_{batt}} \int (\mathrm{i}_{batt}^{ref} - \mathrm{i}_{batt})\,\mathrm{dt} + k_P^{i_{batt}} (\mathrm{i}_{batt}^{ref} - \mathrm{i}_{batt}) \\ U_3 = k_I^{V_{bus}} \int (\mathrm{V}_{bus}^{ref} - V_{bus})\,\mathrm{dt} + k_P^{V_{bus}} (\mathrm{V}_{bus}^{ref} - V_{bus}) \\ U_4 = k_I^{V_{SC}} \int (\mathrm{V}_{SC}^{ref} - V_{SC})\,\mathrm{dt} + k_P^{V_{SC}} (\mathrm{V}_{SC}^{ref} - V_{SC}) \end{cases} \tag{13}$$

With $k_I^{i_{SC}}$, $k_P^{i_{SC}}$ the supercapacitor current controller's integral and proportional gains and i_{SC}^{ref}, i_{SC} the supercapacitor reference and measured current. $k_I^{i_{batt}}$, $k_P^{i_{batt}}$ the battery controller's integral and proportional gains and i_{batt}^{ref}, i_{batt} the battery reference and measured current. $k_I^{V_{bus}}$, $k_P^{V_{bus}}$ the DC bus controller's integral and proportional gains and V_{bus}^{ref}, V_{bus} the DC bus reference and measured voltage. $k_I^{V_{SC}}$, $k_P^{V_{SC}}$ the supercapacitor voltage controller's integral and proportional gains and V_{SC}^{ref}, V_{SC} the supercapacitor's reference and measured voltage.

3.2. SSA Optimizer

Salp swarm algorithm (SSA) is a meta-heuristic algorithm who is created by Mirjalili [18]. This optimizer is inspired by the movement of the salps on the ocean. It meanly characterized by its fast resolving and its high precision. In the agent set, there are two types of agents: leader and followers, the movement of each one can be modelled as

Preprints (www.preprints.org) | NOT PEER-REVIEWED | Posted: 19 January 2021 doi:10.20944/preprints202101.0371.v1

$$LP(\mathrm{k}) = \begin{cases} FP(\mathrm{k}) + \mathrm{c}_1((\mathrm{ub} - \mathrm{lb})\,\mathrm{c}_2 + \mathrm{lb}) & if \quad \mathrm{c}_3 < 0.5 \\ FP(\mathrm{k}) - \mathrm{c}_1((\mathrm{ub} - \mathrm{lb})\,\mathrm{c}_2 + \mathrm{lb}) & if \quad \mathrm{c}_3 > 0.5 \end{cases} \tag{14}$$

$$c_1 = 2e^{-(4k/T_{\max})^2} \tag{15}$$

Where LP(k) is the leader position at the iteration k, FP(k) is the food position (the target) at the iteration k, c2 and c3 are random variables [0,1]. ub and lb are the upper and lower search space limits. The follower's movement can be modelled as

$$FP_i(\mathrm{k}) = 0.5(FP_i(\mathrm{k}-1) + FP_{i-1}(\mathrm{k})) \tag{16}$$

Where LPi(k) is the i-th follower position, it updates its position according to its position and the precedent agent position.

The objective function is to minimize the voltage reference and ensure safe operating to the HPS. The objective function can be written as function the error as

$$objFun = \min(\int_0^t \varepsilon dt) \tag{17}$$

For the HPS, there are four errors, the bus voltage error, the supercapacitor error, the battery current error and the supercapacitor error

$$\begin{cases} \varepsilon_{V_{bus}} = V_{bus}^{ref} - V_{bus} \\ \varepsilon_{V_{SC}} = V_{SC}^{ref} - V_{SC} \\ \varepsilon_{i_{batt}} = i_{batt}^{ref} - i_{batt} \\ \varepsilon_{i_{SC}} = i_{SC}^{ref} - i_{SC} \end{cases} \tag{18}$$

4. Simulation Results

In this part, MATLAB-Simulink is used to validate the proposed EMS. The system parameters are summarized in Table. 1.

Table 1. Simulation parameters.

Parameters	Value
R_1,R_2 (Ω)	0.1
L_1,L_2 (mH)	2
$V_{SC\ ref}$ (V)	200
$V_{bus\ ref}$ (V)	400
C_{SC} (F)	120
C_{bus} (μF)	2000
C_{batt} (Ah)	1500

To validate the performance of the proposed EMS, the load profile illustrated in Figure 8 is used. The simulation results are given in Figure 9. In the beginning, the load is positive, which supplied by the battery, then it will be negative, the battery will charge itself. The battery SoC is given in Figure 10.

Preprints (www.preprints.org) | NOT PEER-REVIEWED | Posted: 19 January 2021 doi:10.20944/preprints202101.0371.v1

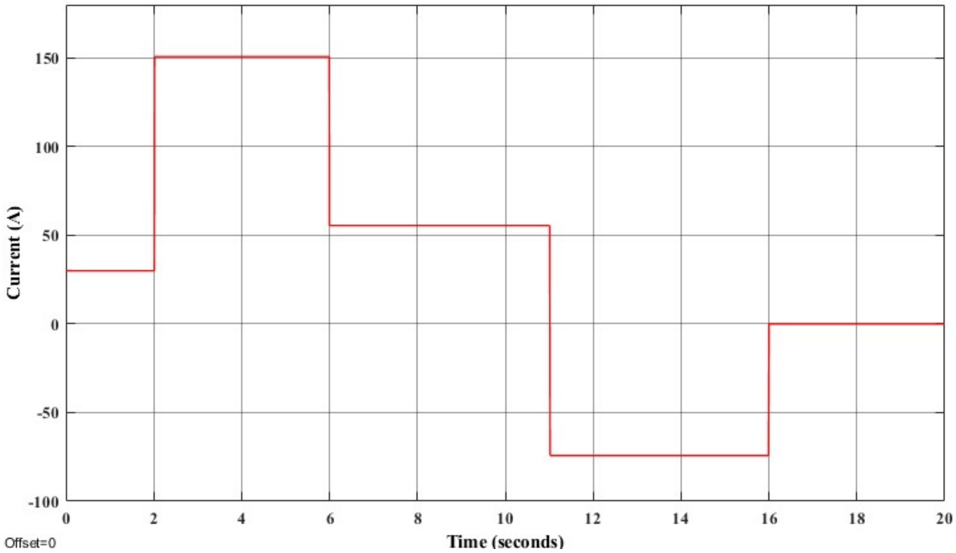

Figure 8. The Proposed Load Profile.

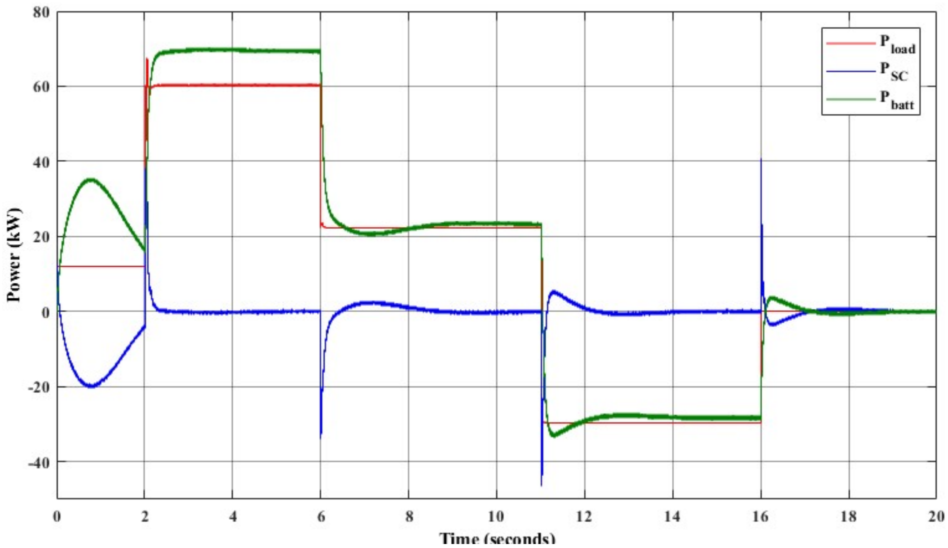

Figure 9. The Simulation Results.

Preprints (www.preprints.org) | NOT PEER-REVIEWED | Posted: 19 January 2021 doi:10.20944/preprints202101.0371.v1

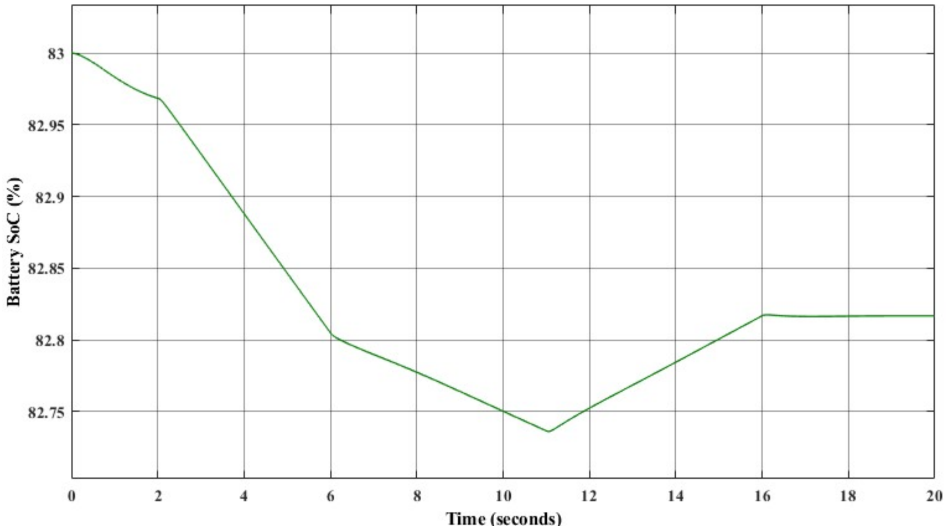

Figure 10. The Battery SoC.

As illustrated in Figure 9, the load is mainly provided by the battery, where the supercapacitor supplies the transitory power, which means that its average power is zero. The Battery charges the supercapacitor to hold its voltage at the reference value. Where the initial supercapacitor voltage is less the reference as illustrated in Figure 11. Thus, the supercapacitor power is negative to charge itself.

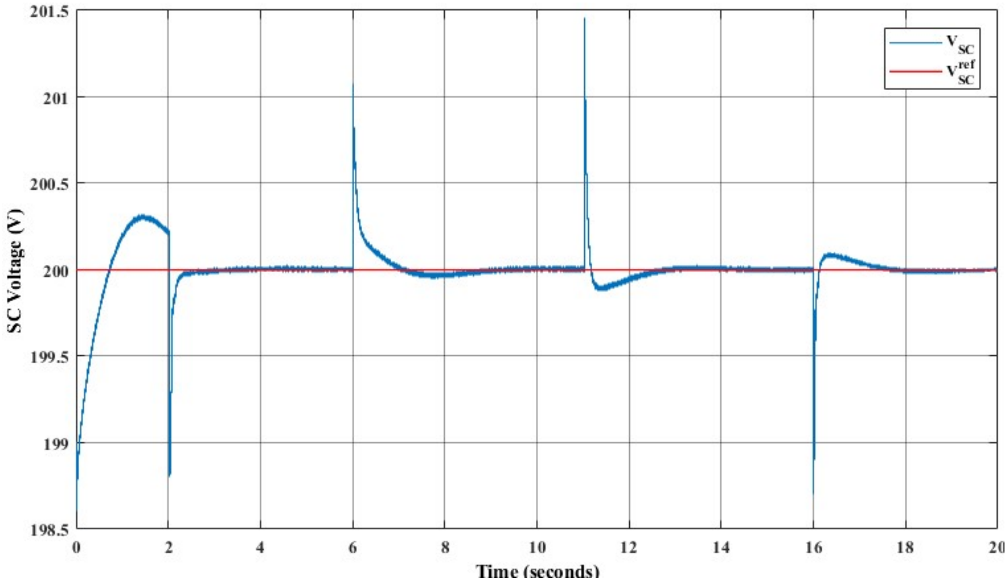

Figure 11. The Supercapacitor Voltage.

The Proposed EMS stabilize the bus voltage against the high steps in the load power. The updating mechanism allows the LQR voltage controller to change its parameters depending on the error between the measured and the reference voltage, which enhances the controller performance. The bus voltage is illustrated in Figure 12.

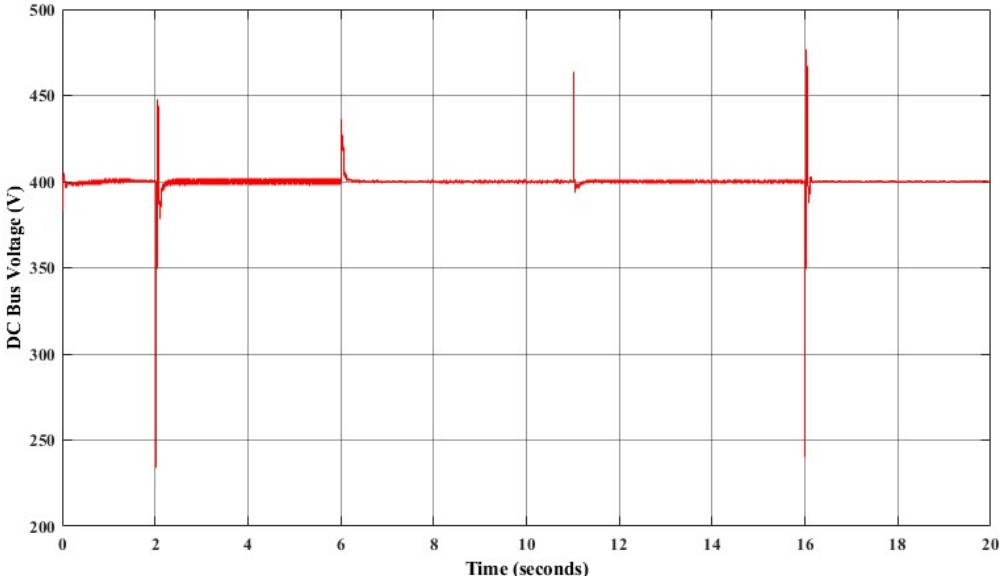

Figure 12. The DC Bus Voltage.

To emulate the real load behavior, the load profile represented in Figure 13 is used. The simulation results are given in Figure 14. The battery SoC is presented in Figure 15.

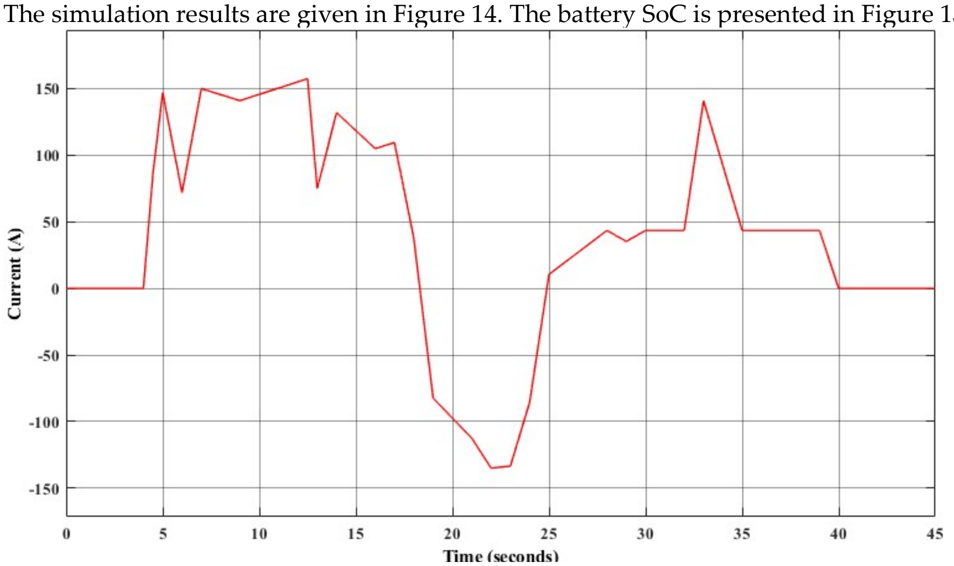

Figure 13. The Second Proposed Load Current.

Preprints (www.preprints.org) | NOT PEER-REVIEWED | Posted: 19 January 2021 doi:10.20944/preprints202101.0371.v1

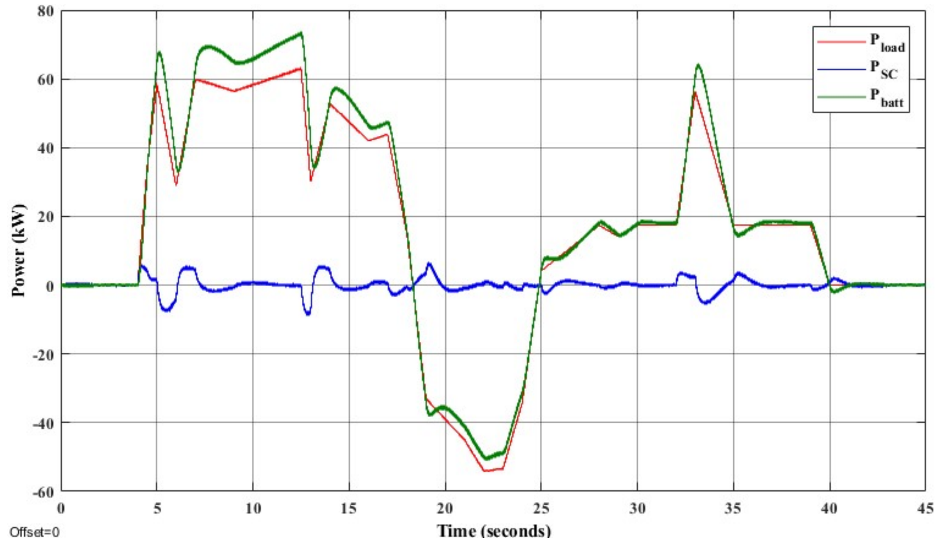

Figure 14. The Simulation Results.

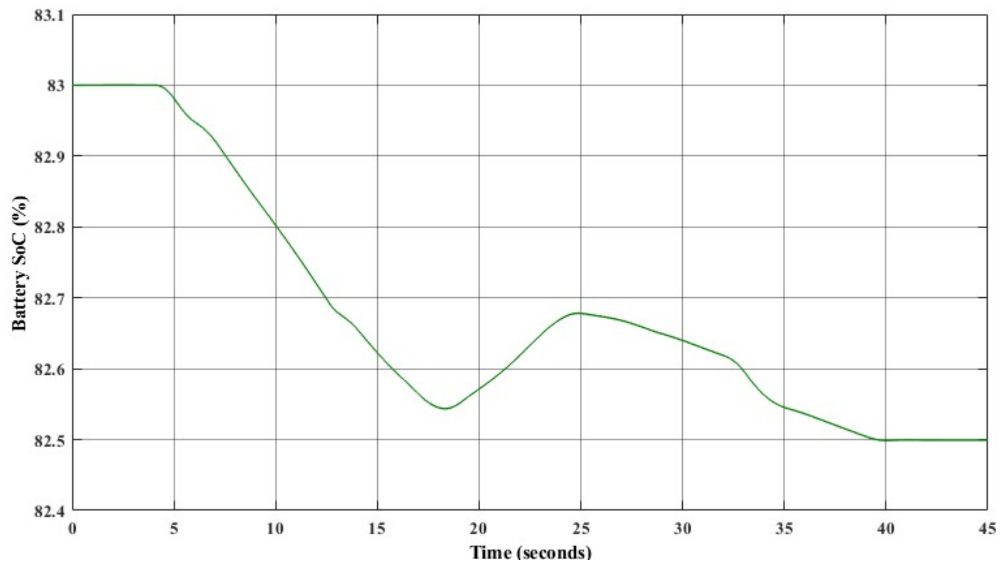

Figure 15. The Battery SoC.

As given in these figures, the load is principally supplied by the battery power, where the fast load variations are supplied by the supercapacitor power.

The Optimal-Adaptive LQR controllers successfully stabilize the bus and the supercapacitor voltage as represented in Figures 16 and 17.

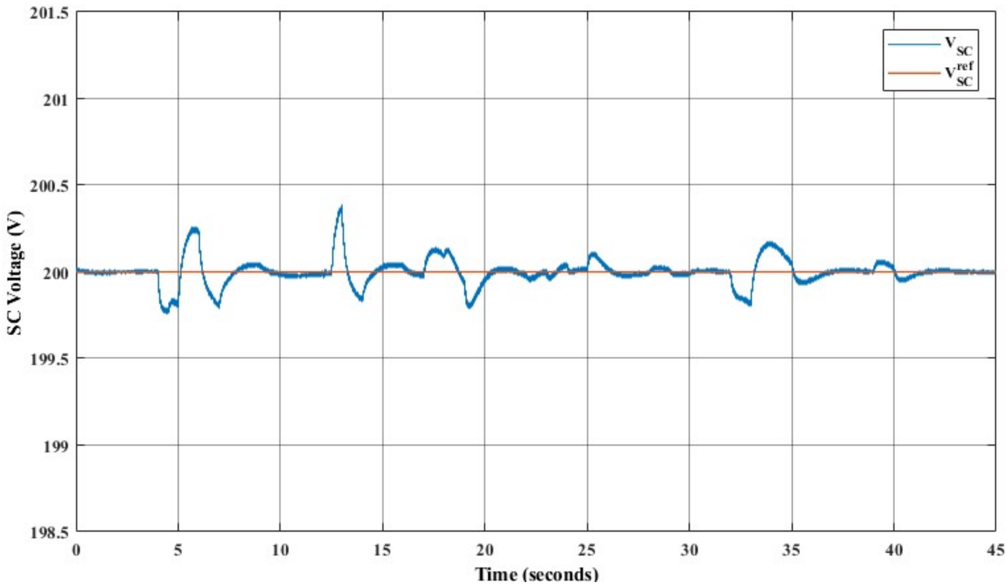

Figure 16. The Supercapacitor Voltage.

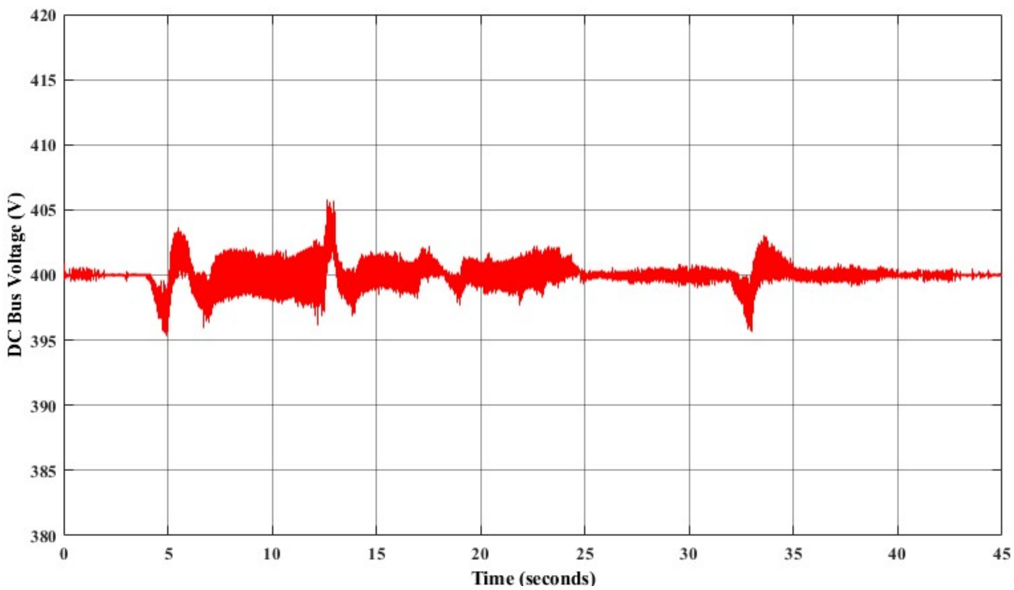

Figure 17. The DC Bus Voltage.

In this case, which emulates the real load demand, the bus voltage is stabilized where the max overshoot voltage is 5.6 V (1.25%) for significant steps in the load (about 60A/s). The voltage ripple is minimized by means of the optimal adaptation process (ΔV = 4V).

5. Conclusions

In this paper, a new optimal energy management strategy regarding a hybrid power system electrified by a battery-supercapacitor and the motivation behind their choice is developed, tested and presented. Given the obtained results, it can be concluded that it is possible to control the converter DC/DC through an elaborated strategy comprised of load following control strategy (LFS) and gain optimization by means LQR-SSA hybrid optimization. This ensures the decrease of battery stress due to supercapacitor providing peak power. Moreover, this strategy satisfies the load respecting the power source dy-

 doi:10.20944/preprints202101.0371.v1

namics and protects the supercapacitor from the deep discharge. Therefore resulting in increased system efficiency and improve the power quality.

Funding: This work was carried out as part of the VEHICLE project, funded by INTERREG V A Upper Rhine Programme (Dpasser les frontires, projet aprs projet), FEDER, and Franco-German regional funds (Bade-Wurtemberg, Rhénanie-Palatinat, and Grand Est).

Conflicts of Interest: The authors declare no conflict of interest

References

1. Paska, J.; Biczel, P.; Kłos, M. Hybrid power systems – An effective way of utilising primary energy sources. *Renew. Energy* **2009**, *34*, 2414–2421, doi:10.1016/j.renene.2009.02.018.
2. Lü, X.; Wu, Y.; Lian, J.; Zhang, Y.; Chen, C.; Wang, P.; Meng, L. Energy management of hybrid electric vehicles: A review of energy optimization of fuel cell hybrid power system based on genetic algorithm. *Energy Convers. Manag.* **2020**, *205*, 112474, doi:10.1016/j.enconman.2020.112474.
3. Sorlei, I.-S.; Bizon, N.; Thounthong, P.; Varlam, M.; Carcadea, E.; Culcer, M.; Iliescu, M.; Raceanu, M. Fuel Cell Electric Vehicles—A Brief Review of Current Topologies and Energy Management Strategies. *Energies* **2021**, *14*, 252, doi:10.3390/en14010252.
4. Shigeta, N.; Hosseini, S.E. Sustainable Development of the Automobile Industry in the United States, Europe, and Japan with Special Focus on the Vehicles' Power Sources. *Energies* **2020**, *14*, 78, doi:10.3390/en14010078.
5. Ou, K.; Yuan, W.-W.; Choi, M.; Yang, S.; Jung, S.; Kim, Y.-B. Optimized power management based on adaptive-PMP algorithm for a stationary PEM fuel cell/battery hybrid system. *Int. J. Hydrogen Energy* **2018**, *43*, 15433–15444, doi:10.1016/j.ijhydene.2018.06.072.
6. Olabi, A.G.; Wilberforce, T.; Abdelkareem, M.A. Fuel cell application in the automotive industry and future perspective. *Energy* **2021**, *214*, 118955, doi:10.1016/j.energy.2020.118955.
7. Ferahtia, S.; Djerioui, A.; Zeghlache, S.; Houari, A. A hybrid power system based on fuel cell, photovoltaic source and supercapacitor. *SN Appl. Sci.* **2020**, *2*, 940, doi:10.1007/s42452-020-2709-0.
8. Xun, Q.; Liu, Y.; Holmberg, E. A Comparative Study of Fuel Cell Electric Vehicles Hybridization with Battery or Supercapacitor. In Proceedings of the 2018 International Symposium on Power Electronics, Electrical Drives, Automation and Motion (SPEEDAM); IEEE, 2018; pp. 389–394.
9. Hemi, H.; M'Sirdi, N.K.; Naamane, A. A new proposed shepherd model of A li-ion open circuit battery based on data fitting. *12th Int. Conf. Integr. Model. Anal. Appl. Control Autom. IMAACA 2019* **2019**, 83–92.
10. Qi, W.; Li, Y.; Li, H.; Wayne, S.W.; Lin, X. The development and numerical verification of a compromised real time optimal control algorithm for hybrid electric vehicle. *J. Power Sources* **2019**, *443*, 227272, doi:10.1016/j.jpowsour.2019.227272.
11. Zhang, Z.; Guan, C.; Liu, Z. Real-Time Optimization Energy Management Strategy for Fuel Cell Hybrid Ships Considering Power Sources Degradation. *IEEE Access* **2020**, *8*, 87046–87059, doi:10.1109/ACCESS.2020.2991519.
12. Hemi, H.; Ghouili, J.; Cheriti, A. A real time fuzzy logic power management strategy for a fuel cell vehicle. *Energy Convers. Manag.* **2014**, *80*, 63–70, doi:10.1016/j.enconman.2013.12.040.
13. Jia, Z.; Jiang, J.; Lin, H.; Cheng, L. A Real-time MPC-based Energy Management of Hybrid Energy Storage System in Urban Rail Vehicles. *Energy Procedia* **2018**, *152*, 526–531, doi:10.1016/j.egypro.2018.09.205.
14. LI, A. Analyse expérimentale et modélisation d ' éléments de batterie et de leurs assemblages : application aux véhicules électriques et hybrides. *Thèse Dr. , Univ. Claude Bernard LYON 1* **2015**.
15. Wang, T.; Li, Q.; Chen, W.; Liu, T. Application of energy management strategy based on state machine in fuel

cell hybrid power system. In Proceedings of the 2017 IEEE Transportation Electrification Conference and Expo, Asia-Pacific (ITEC Asia-Pacific); IEEE, 2017; pp. 1–5.

16. Zhang, Q.; Deng, W.; Zhang, S.; Wu, J. A Rule Based Energy Management System of Experimental Battery/Supercapacitor Hybrid Energy Storage System for Electric Vehicles. *J. Control Sci. Eng.* **2016**, *2016*, 1–17, doi:10.1155/2016/6828269.
17. Hemi, H.; Ghouili, J.; Cheriti, A. A real time fuzzy logic power management strategy for a fuel cell vehicle. *Energy Convers. Manag.* **2014**, *80*, 63–70, doi:10.1016/j.enconman.2013.12.040.
18. Mirjalili, S.; Gandomi, A.H.; Mirjalili, S.Z.; Saremi, S.; Faris, H.; Mirjalili, S.M. Salp Swarm Algorithm: A bio-inspired optimizer for engineering design problems. *Adv. Eng. Softw.* **2017**, *114*, 163–191, doi:10.1016/j.advengsoft.2017.07.002.